

Science in the Art of the Master Bizen Potter

YOSHIHIRO KUSANO,^{*,†} MINORU FUKUHARA,[‡] JUN TAKADA,[§]
AKIRA DOI,[†] YASUNORI IKEDA,[⊥] AND MIKIO TAKANO^{||}

[†]Department of Fine and Applied Arts, Kurashiki University of Science and the Arts, 2640 Nishinoura, Tsurajima-cho, Kurashiki-shi, Okayama 712-8505, Japan, [‡]Department of Applied Chemistry, Okayama University of Science, 1-1 Ridai-cho, Kita-ku, Okayama 700-0005, Japan, [§]Department of Applied Chemistry, Okayama University, 3-1-1 Tsushima-naka, Kita-ku, Okayama 700-8530, Japan, [⊥]Research Institute for Production Development, 15 Shimogamo Morimoto-cho, Sakyo-ku, Kyoto 606-0805, Japan, and ^{||}Institute for Integrated Cell-Material Sciences, Kyoto University, Yoshida Ushinomiya-cho, Sakyo-ku, Kyoto 606-8501, Japan

RECEIVED ON JULY 5, 2009

CONSPECTUS



Bizen stoneware, with the characteristic reddish hidasuki or “fire-marked” pattern, is one of Japan’s best known traditional ceramic works of art. The means of creating and controlling the various hues of the hidasuki pattern has remained a mystery to outsiders for about a thousand years; the methods were known only to master potters who served under generations of master potters before them. In this Account, we present the results of 30 years of study in which we investigated the microstructure and color-formation process in Bizen stoneware.

We discovered that the hidasuki pattern results from the precipitation of corundum ($\alpha\text{-Al}_2\text{O}_3$) and the subsequent epitaxial growth of hematite ($\alpha\text{-Fe}_2\text{O}_3$) around it in a $\sim 50\text{-}\mu\text{m}$ -thick liquid specifically formed in the ceramic surface. The epitaxial composites include hexagonal plate-like $\alpha\text{-Fe}_2\text{O}_3/\alpha\text{-Al}_2\text{O}_3/\alpha\text{-Fe}_2\text{O}_3$ sandwiched particles and also surprisingly beautiful flower-like crystals, centered by hexagonal corundum crystals and decorated by several hexagonal hematite petal crystals. Bizen stoneware is produced from a unique clay that can only be mined from the Bizen area of Okayama Prefecture, Japan. The clay has an unusually high Fe content compared with the traditional porcelain clay, as well as Si, Ca, Mg, and Na. Prior to firing, the Bizen works are wrapped in rice straw that was used originally as a separator to prevent adhesion. The hidasuki pattern only appears where the rice straw is in direct contact with the clay; the rice straw supplies potassium, which reduces the melting point of the ceramic surface, thereby converting the contact area into a site for these reactions to take place. The effect is almost accidental and is produced without the aid of any artificial glazing and enameling. An unexpected variety of substances, including metallic iron coated by graphite, Fe_3P , and $\varepsilon\text{-Fe}_2\text{O}_3$, were also found to appear at low oxygen partial pressures.

Many of the techniques used by master potters are passed down through an apprenticeship system; an unfortunate consequence is that they are poorly documented. Moreover, the masters of these techniques are often unaware of the underlying chemical reactions that take place. Chemical studies of traditional processes can provide new inspiration to artists, allowing them to control the various factors and thus produce new works, and perhaps new functional materials. We studied the process of creating Bizen stoneware and then mimicked the color-producing process under controlled laboratory conditions, demonstrating the possibilities of the endeavor.

Introduction

Traditional ceramic products, in the form of earthenware, pottery, stoneware, and porcelain, have been produced by Japanese artists for thousands of years. In fact, one of the oldest pieces of pottery ever to be found was located in Japan and estimated to be over 16 000 years old.¹ Today, traditional ceramic production areas are located throughout Japan, and over 2 600 000 amateur artists enjoy making ceramic bowls, plates, cups, and other utensils on their weekends.²

Unfortunately, many of the techniques used by master potters are passed down from generation to generation through an apprenticeship system and are thus poorly documented. In addition, even the masters of these techniques are unaware of the underlying chemical reactions that take place, so many years of experience, as well as a great deal of trial and error, are required before they can be expected to select the right clay composition, firing temperature, cooling rate, and oxygen partial pressure in the kiln for a particular effect.

We believe that chemical studies of traditional processes can provide new inspiration to artists by allowing them to control the various factors and thus produce new and exciting works. We also hope that through a greater understanding and documentation of the mechanisms and processes involved in creating traditional arts, we can preserve them for future generations to enjoy. It should not be overlooked that chemical studies of traditional arts can also provide chemists with new concepts to develop novel functional materials.

This Account summarizes over 30 years of work to understand the formation of the characteristic reddish-color pattern in Bizen stoneware, which is one of Japan's best known traditional ceramic works of art. Through this study, we identify a novel sandwich-like crystal structure of corundum ($\alpha\text{-Al}_2\text{O}_3$) and hematite ($\alpha\text{-Fe}_2\text{O}_3$) and also reveal an interesting iron oxide crystal growth with useful magnetic properties.

History of Bizen Stoneware

Japan is a nation renowned for its ability to borrow ideas from other nations and then modify and improve on them in the creation of original products. Therefore, it is not surprising to find that one of Japan's best-loved traditional ceramic products, Bizen stoneware, was inspired by the unglazed stoneware called Sue-ware using techniques from the Korean peninsula in the fifth century.

Bizen stoneware is a surprisingly simple unglazed ceramic that expresses two deep and important Japanese concepts of *wabi* (a display of richness and beauty in simplicity and poverty) and *sabi* (an aesthetic sense of loneliness). Visitors to the country will immediately recognize these concepts not only in



FIGURE 1. Hidasuki bowl used for tea ceremonies.

Bizen stoneware, but also in flower arrangements, tea houses, Japanese gardens, and even music.

Bizen stoneware grew in popularity after it was adopted by the great tea-master Sen no Rikyu (1522–1591), who used it as part of his tea ceremony during the Azuchi-Momoyama period (1573–1603). Unfortunately, after the death of Sen no Rikyu, Japanese tastes began to change, especially due to the growth in popularity of the blue/white porcelain produced in China during the Ming dynasty (1365–1644), and the overglazed porcelain as produced by Kakiemon in the Edo period (1603–1867). Such was the popularity of the red/white Kakiemon-style porcelain, which was exported to Europe, that porcelain production in Japan increased rapidly, leaving Bizen stoneware to be used mainly for daily use by Japanese families. Fortunately, interest in Bizen stoneware was revived during the Showa era (1926–1989) when the great potter Toyo Kaneshige, who himself became a national treasure in 1956, reproduced the aesthetic properties of the Azuchi-Momoyama period Bizen stoneware. Today, Bizen stoneware continues to be one of the most popular traditional Japanese ceramics both in Japan and elsewhere.

Characteristics of Bizen Stoneware

Bizen stoneware is often described as the art of clay and flame because the potter can control the firing conditions to produce a wide array of colors on the surface, from red, orange, purple, and yellow to black, silver, and gold, without using any artificial glazing or enameling. Of these colors, one of the most characteristic of the art is the *hidasuki* or “fire-marked” pattern (Figure 1). This color appears almost accidentally on the surface of the stoneware where the clay is in contact with rice straw that is used as a separator to prevent adhesion during firing (Figure 2). In fact, these coloring processes, including



FIGURE 2. Green Bizen stoneware inside a kiln prior to firing.

hidasuki, are even referred to as *yohen* or “kiln accident” by the potters themselves.

Potters have long known that two factors influence the *hidasuki* color, the clay and the rice straw. Bizen stoneware can only be produced from clay that is mined from rice paddies in the Bizen area of Okayama Prefecture, Japan.³ The chemical composition of Bizen clay is shown in Table 1. On the other hand, the rice straw contains potassium and is reduced to white ash consisting mainly of cristobalite (SiO_2) during firing (ca. 13 wt % K_2O in the ash). This remains on the surface and clearly marks the areas where the *hidasuki* color appears (Figure 3a,b).

Our early work on the appearance of the *hidasuki* color revealed that it was due to the formation of hematite particles.^{4–9} Hematite is also used as the overglaze for the red/white Kakiemon-style porcelain. The color of hematite particles changes depending on their size, from small particles with a vermilion color to large particles that appear black. It is also known that the heating of hematite crystals above 800 °C leads to aggregation and growth.^{10,11} Therefore, if the formation mechanism of hematite can be understood, it should be possible to control the color of the crystals and thus the *hidasuki* pattern.

Hematite Formation Mechanism

To investigate the formation mechanism of hematite, pellets (20 mm in diameter and ca. 2 mm in thickness) of the Bizen clay with and without rice straw were heated to 1250 °C in air and then cooled at different rates. Figure 4 shows the results of the study. Sample NR800/1 (a) was heated to 1250 °C without rice straw and then cooled to 800 °C at a rate of 1 °C/min. Samples R1250Q, R800/10, and R800/1 were all completely covered with approximately 0.4 g of dried rice straw (3 mm in diameter and 2.5 cm in length) before heat-

ing to 1250 °C and then were either quenched in air (b) or cooled to 800 °C at a rate of 10 (c) or 1 °C/min (d) in air.

Unsurprisingly, the *hidasuki* color did not appear when rice straw was not employed. Sample NR800/1 (a), for example, appears ochreous with a rough surface. The color of other samples heated without rice straw was the same, regardless of the cooling rate (not shown). According to X-ray diffractometry (XRD) measurements, NR800/1 contains mainly quartz (SiO_2), cristobalite, and mullite ($(\text{Al,Fe})_6\text{Si}_2\text{O}_{13}$ with $\text{Al/Fe} \approx 9/1$)^{12–15} on the surface. The ochreous color is caused by the iron-substituted mullite, which hereafter is referred to as mullite for the sake of simplicity.

Sample R1250Q (b) also has a similar color to sample NR800/1, despite the presence of rice straw during the heating process. Sample R1250Q has a lustrous surface due to the formation of a glassy phase during heating. This vitrification is caused by the potassium contained in the rice straw, which lowers the melting point of the stoneware surface to a depth of $\sim 50 \mu\text{m}$.¹⁶ Potassium supplied by rice straw is an essential element for vitrification.

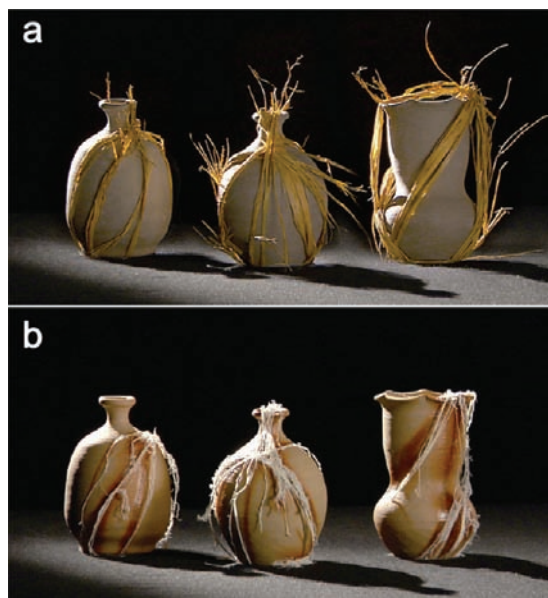
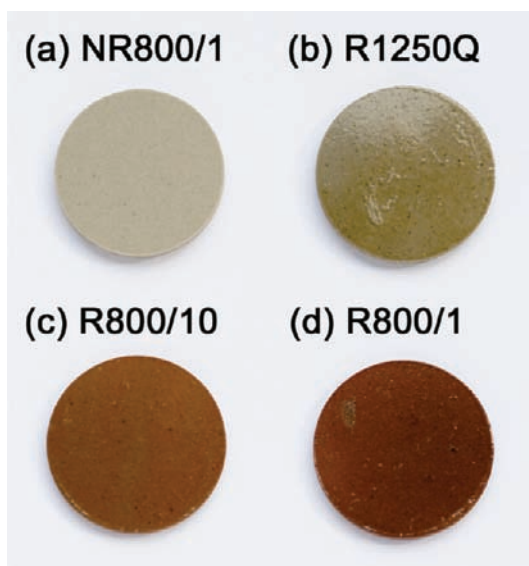
In contrast, the R800/10 and R800/1 samples have the characteristic reddish *hidasuki* color, which reveals that the cooling rate is also an important factor in the formation of the *hidasuki* color. XRD measurements showed that the surface of the R800/10 and R800/1 samples contained quartz, cristobalite, hematite, and corundum.⁴ As the cooling rate was decreased, the peak intensity of hematite increased. Scanning electron microscope (SEM) observations revealed that hexagonal plate-like iron-rich grains were present at the surfaces, after treatment with 47% hydrofluoric acid for 3 min to remove a glassy phase in which the target crystalline materials were embedded. The size of these hexagonal grains also increased as the cooling rate decreased. These results led us to conclude that the coloring material was hexagonal plate-like hematite that precipitated in the glassy phase during the cooling process.^{8,9}

When we revisited the *hidasuki* problem in 2002, more detailed analyses of the formation process were conducted using transmission electron microscopy (TEM) and electron diffractometry (ED) measurements. These experiments revealed that corundum was a key component in the formation of *hidasuki*.^{16–18} Figure 5 shows TEM images of the crystalline phases obtained from the sample surfaces shown in Figure 4. The samples for these observations were prepared by treating the pellet surface with 47% hydrofluoric acid for 5 min to remove a glassy phase in which the target crystalline materials were embedded. The crystals were dispersed in carbon tetrachloride using ultrasonic waves and then collected on a

TABLE 1. Chemical Composition (wt %) of the Bizen Clay

SiO ₂	TiO ₂	Al ₂ O ₃	Fe ₂ O ₃	CaO	MgO	MnO	K ₂ O	Na ₂ O	P ₂ O ₅	Ig. loss
63.51	0.69	21.61	2.77	0.56	0.66	0.03	2.05	0.51	0.04	7.57

microgrid. Figure 5a shows that the main crystalline phase in NR800/1 is needle-like mullite crystals that grow along the *c*-axis in a {110}-faceted manner. On the other hand, Figure 5b shows R1250Q to contain large plate-like corundum particles of approximately 1 μm in size. Corundum usually has a

**FIGURE 3.** External appearance of Bizen Stoneware (a) before and (b) after firing at 1250 °C in air with rice straw.**FIGURE 4.** Colors of samples heated with or without rice straw: (a) sample NR800/1 was heated without rice straw at 1250 °C in air and then cooled to 800 °C at a rate of 1 °C/min; samples of R1250Q, R800/10, and R800/1 were heated with rice straw on the surface in air at 1250 °C and then (b) quenched, (c) cooled to 800 °C at a rate of 10 °C/min, or (d) cooled to 800 at 1 °C/min.

hexagonal rod-like shape but can form a hexagonal plate-like shape in the presence of additional elements, such as Si, Ca, Mg, and Na,^{19–21} which are all contained in Bizen clay (Table 1). The inset shows an electron diffraction (ED) pattern of the crystal, which indicates that the growth proceeded preferentially in the basal plane.

TEM images of the reddish R800/10 and R800/1 samples are shown in Figure 5c,d, respectively. Energy-dispersive spectroscopy (EDS), XRD, and ED measurements show that the relatively large plate-like particles shown in Figure 5c are corundum (labeled C), and the smaller, dark plate-like particles are hematite (labeled H). The EDS results indicate that iron is concentrated in the hematite particles, some of which are labeled C+H (Figure 5d). The reason for the C+H labeling will become apparent shortly.

Figure 6 shows TEM images of the corundum and hematite particles in sample R800/10. In Figure 6a, a corundum crystal of approximately 1.5 μm in width is attached to hematite crystals of approximately 0.5 μm or less in width. It is interesting to note that both corundum and hematite crystallize in the same $R\bar{3}c$ structure with $a = 0.4758$ nm and $c = 1.2991$ nm (JCPDS No. 10-0173) and $a = 0.5036$ nm and $c = 1.3749$ nm (JCPDS No. 33-0664), respectively. The ED patterns of hexagonal symmetry shown in the first inset of Figure 6a reveal that the crystal directions are the same, indicating an epitaxial relation between these phases.

The second inset in Figure 6a shows an enlarged TEM image of the *c*-plane of the corundum crystal. The *c*-plane is very smooth, but the edges of the growth front seem to be reactive with kinks and steps. These sites probably provide the hematite nucleation sites, and the dislocations in the hematite crystals are caused by the lattice misfit.

Figure 6b shows a cross sectional $[\bar{1}2\bar{1}0]$ TEM image of a thin corundum crystal embedded in a hematite crystal. These structures give rise to the dark, iron-rich particle images observed earlier, which were initially thought to be only composed of hematite. As a result, these are labeled as C+H in Figure 5d, corresponding to this unique $\alpha\text{-Fe}_2\text{O}_3/\alpha\text{-Al}_2\text{O}_3/\alpha\text{-Fe}_2\text{O}_3$ sandwich structure.

From the above observations, we can now conclude the mechanism of formation of the *hidasuki* pattern. First, reaction of the components in Bizen clay with potassium supplied by the rice straw at 1250 °C results in the formation of three

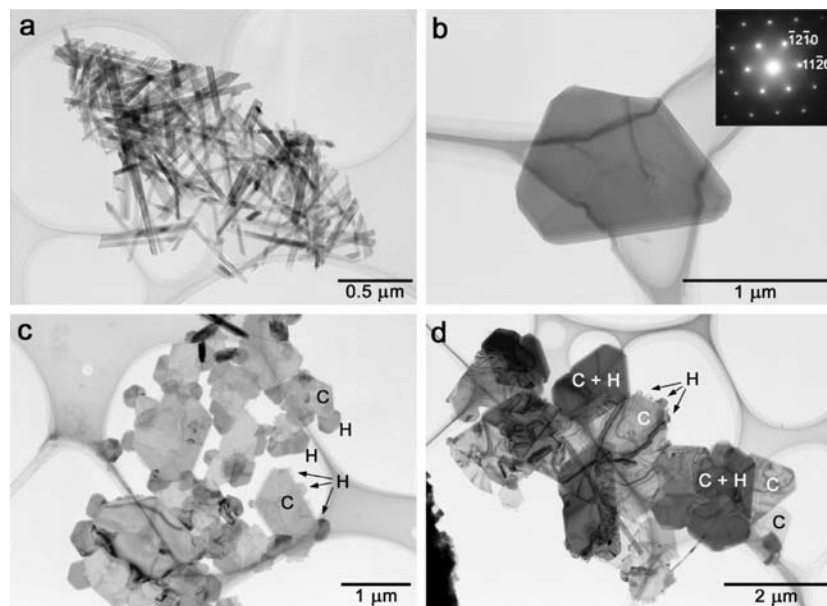


FIGURE 5. TEM images of the (a) NR800/1, (b) R1250Q, (c) R800/10, and (d) R800/1 samples.

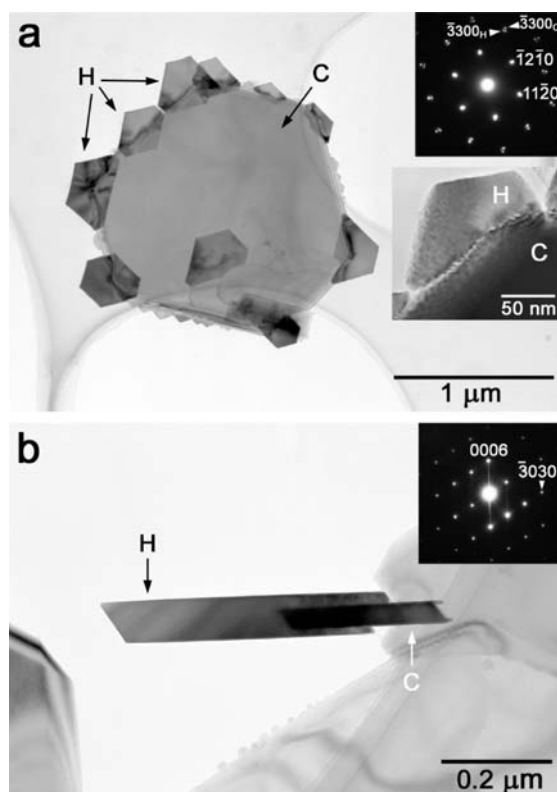


FIGURE 6. TEM images and ED patterns of the R800/10 sample. The ED pattern shown in panel a is the [0001] zone axis of corundum and hematite. Image b is a cross-sectional [1210] TEM image showing a part of the $\alpha\text{-Fe}_2\text{O}_3/\alpha\text{-Al}_2\text{O}_3/\alpha\text{-Fe}_2\text{O}_3$ sandwich-like structure.

phases, a liquid phase, SiO_2 , and corundum. Second, during the cooling process, hematite crystals grow around the corundum particles, creating the characteristic reddish-colored sand-

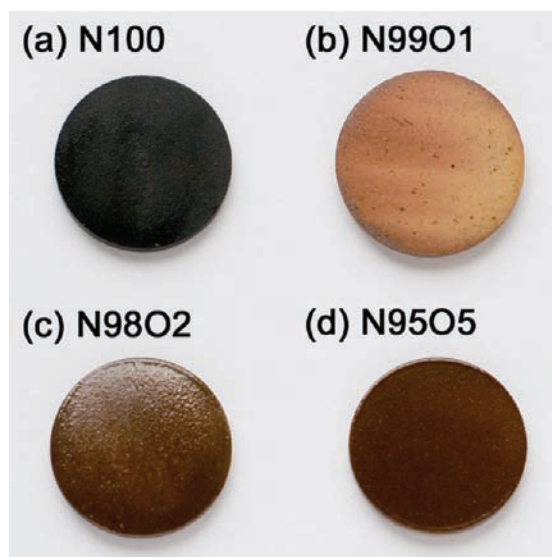


FIGURE 7. Colors of clay pellets covered with rice straw and heated at 1250 °C in N_2/O_2 gas mixtures of (a) 100/0 (N100), (b) 99/1 (N99O1), (c) 98/2 (N98O2), and (d) 95/5 vol % (N95O5). wick-like structure.¹⁶ Corundum and hematite are also found not only in *hidasuki* but also in other traditional reddish ceramics such as terra sigillata.^{22,23}

Effect of Oxygen Partial Pressure

Experiments were then conducted to determine the influence of oxygen partial pressure on the formation of *hidasuki*.²⁴ Figure 7 shows the colors of sample surfaces heated with rice straw at 1250 °C in various flowing gas mixtures of N_2/O_2 of 100/0 (N100) (Figure 7a), 99/1 (N99O1) (Figure 7b), 98/2 (N98O2) (Figure 7c), and 95/5 vol % (N95O5) (Figure 7d), where the sample names reflect the partial oxygen pressures

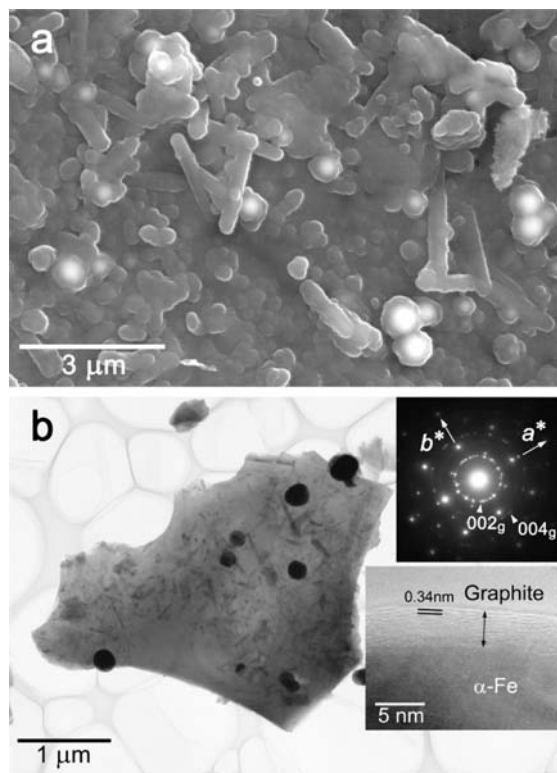


FIGURE 8. SEM image of the N100 surface treated with 47% HF (a) and TEM image of a fragment scraped from the inside of N100 (b). The stick-like particles seen in both images are mullite, while round particles in image a are Fe_3P . Spherical particles in image b embedded in a glassy matrix are $\alpha\text{-Fe}$. The insets in b show a typical ED pattern of an $\alpha\text{-Fe}$ particle and an enlarged TEM image of an $\alpha\text{-Fe}$ particle surface, showing that $\alpha\text{-Fe}$ particles are covered by a thin graphite layer.

used. All the samples were heated at 1250 °C, and then cooled to 800 °C at a rate of 1 °C/min.

Sample N100 appears black (Figure 7a), while a slight increase in oxygen content dramatically changes the appearance to a yellowish color in N9901 (Figure 7b). The characteristic *hidasuki* color is revealed in the N9802 and N9505 samples when the oxygen content is increased to 2 vol % or higher (Figure 7c,d). The color tone becomes deeper as the oxygen partial pressure increases, which demonstrates that the *hidasuki* color can be controlled not only by changes in the cooling rate but also by changes in the oxygen content.

Figure 8 shows an SEM image of the N100 surface after treatment with 47% hydrofluoric acid (a) and a TEM image of a fragment scraped from the inside of N100 (b). Stick-like particles seen in both images are mullite. Round particles in image a are, to our surprise, identified as iron phosphide (schreibersite, Fe_3P) particles. Considering the fact that rice straw heated at 1000 °C leaves 0.89 wt % of P_2O_5 in its residual ash, it could be concluded that schreibersite is formed through reactions of the phosphorus from the rice straw and iron from the Bizen clay. In Figure 8b, another

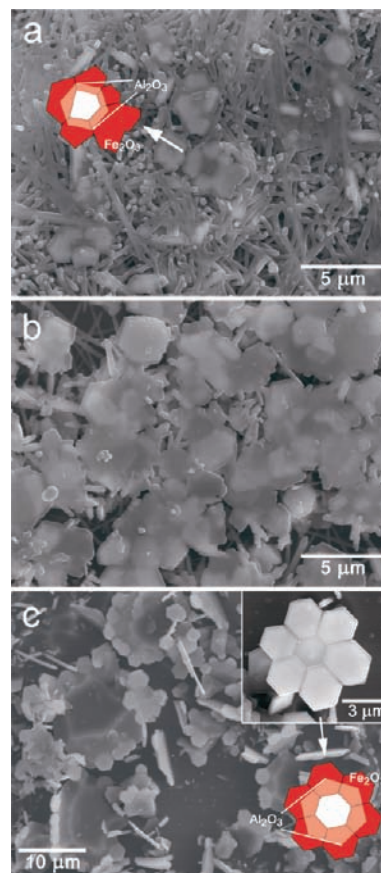


FIGURE 9. SEM images of the (a) N9901, (b) N9802, and (c) N9505 surfaces. Insets show schematic illustrations of composite particles of corundum and hematite.

kind of spherical particles of ca. 0.4 μm in diameter are embedded in the glassy matrix. Phosphorus was absent in these spherical particles, despite their morphological similarity to the Fe_3P particles. The ED pattern shown in the inset clearly indicates $\alpha\text{-Fe}$ but contains additional spots designated as 002_g and 004_g . These spots are assigned to the (002) and (004) reflections from graphite. The 0.34 nm-spaced lattice fringes in the magnified image in Figure 8b correspond to the (002) planes of graphite. The rice straw can be a carbon source, but the clay itself also can be because clay naturally contains a small amount of organic substances.^{3,16} These Fe_3P and $\alpha\text{-Fe}$ covered by graphite are blackish in color, which gives rise to the appearance shown in Figure 7a. It has been thought that the black color of Bizen stoneware prepared in a reducing atmosphere is due to the formation of magnetite (Fe_3O_4). It should be noted that schreibersite and $\alpha\text{-Fe}$ covered by graphite are formed through carbothermal reductions occurring on the combustion of rice straw, because these phases were not produced without rice straw.

Figure 9a shows stick-like mullite particles and $\alpha\text{-Fe}_2\text{O}_3/\alpha\text{-Al}_2\text{O}_3$ composite particles in the N9901 sample. Figure 9a also includes an illustration of one of the large

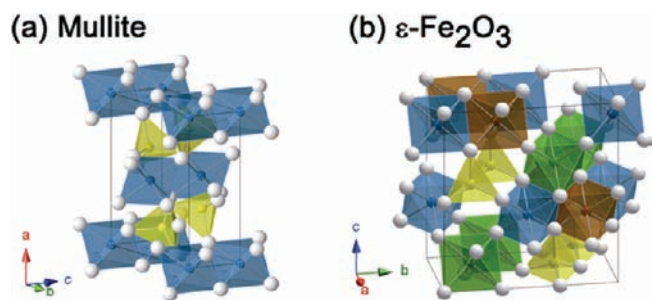


FIGURE 10. Schematic representation of the crystal structures of (a) mullite and (b) ϵ - Fe_2O_3 . In panel a, the AlO_6 octahedra are colored blue and the $(\text{Al,Si})\text{O}_4$ tetrahedra yellow. In panel b, the FeO_6 octahedra are colored blue, green, and brown to indicate their crystallographic difference, and the FeO_4 tetrahedra are colored yellow.

particles, in which the red, white, and pink colors correspond to hematite, corundum, and corundum sandwiched by hematite, respectively. Figure 9b shows that the number of composite particles is significantly increased as the oxygen content increases. At an oxygen content of 5 vol % (Figure 9c), beautiful flower-like crystal structures bloom across the surface of the N9505 sample, which are composed of colorless hexagonal corundum particle centers (ca. $14 \mu\text{m}$ wide and $0.4 \mu\text{m}$ thick) decorated by hexagonal reddish hematite petals (ca. $3 \mu\text{m}$ wide and $0.5 \mu\text{m}$ thick). The corundum particles in Figure 9c are more than three times larger than those formed in air and are therefore too large to be wholly covered by the hematite.

Epitaxial Crystal Growth of Iron Oxide, ϵ - Fe_2O_3

Another very interesting epitaxial crystal growth of iron oxide, ϵ - Fe_2O_3 , on mullite was also found in the N9901 and N9802 samples.²⁵ The structural features of ϵ - Fe_2O_3 and mullite were compared. The iron-substituted mullite in the present samples has an orthorhombic unit cell of $Pbam$ with $a_m = 0.7553 \text{ nm}$, $b_m = 0.7704 \text{ nm}$, and $c_m = 0.2894 \text{ nm}$, in which chains made of edge-sharing AlO_6 octahedra run along the c_m -axis at each corner and at the center, as illustrated in Figure 10a. These chains are linked to $(\text{Al,Si})\text{O}_4$ tetrahedra through corner sharing. In the orthorhombic unit cell of ϵ - Fe_2O_3 ($Pna2_1$, $a_\epsilon = 0.5095 \text{ nm}$, $b_\epsilon = 0.8789 \text{ nm}$, and $c_\epsilon = 0.9437 \text{ nm}$), triple chains composed of edge-sharing FeO_6 octahedra run along the a_ϵ -axis. These chains are connected to each other at shared corners of the FeO_6 octahedra, and the resulting one-dimensional cavities are occupied by chains of corner-sharing FeO_4 tetrahedra (Figure 10b). The c_m -axis length of 0.2894 nm is equal to the Al–Al distance of a pair of edge-sharing octahedra. On the other hand, the near-neighboring FeO_6 octahedra in ϵ - Fe_2O_3 are paired along the b_ϵ -axis in the same

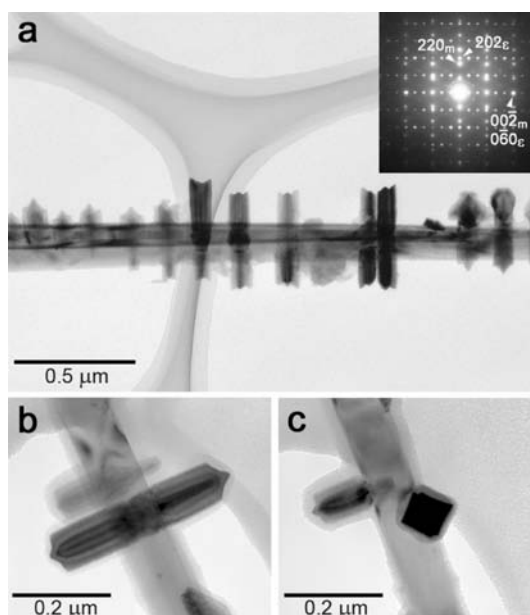


FIGURE 11. TEM images of ϵ - Fe_2O_3 particles attached to mullite (horizontal crystals in image a) in N9901. Images b and c are the same ϵ - Fe_2O_3 particles observed from different angles, showing that ϵ - Fe_2O_3 has a square columnar shape.

edge-sharing manner as that in mullite. The Fe–Fe spacing is almost 0.29 nm for all the combinations of FeO_6 octahedra, which is equal to one-third of the b_ϵ -axis length of 0.8789 nm . Mixing of octahedral and tetrahedral units and their linkage through corner sharing is common to these oxides; however, the overall arrangements of these polyhedra are rather different. These phases are connected epitaxially as described below.

Figure 11 shows TEM images of single-crystalline ϵ - Fe_2O_3 particles with prismatic ends (see Figure 11b) grown on the $\{110\}$ -faceted stick-like mullite crystals in N9901. Figure 11b,c indicates that ϵ - Fe_2O_3 has a square columnar shape ca. $0.1 \times 0.1 \times 0.5 \mu\text{m}^3$ in size. The ED pattern of the inset in Figure 11a indicates the crystallographic relation between ϵ - Fe_2O_3 and mullite, which shows that the $[1\bar{1}0]$ zone axis for mullite corresponds to the $[\bar{1}01]$ zone axis for ϵ - Fe_2O_3 . The crystallographic relations deduced here are $c_m // b_\epsilon$ and $(110)_m // (101)_\epsilon$, which are consistent with the numerical relations of $3c_m \approx b_\epsilon$ and $5d_{(110)_m} \approx 6d_{(101)_\epsilon}$. The ϵ - Fe_2O_3 crystals grow along the a_ϵ -axis in a principally $\{011\}_\epsilon$ -faceted square columnar shape.

ϵ - Fe_2O_3 remarkably changes its crystal shape and size and the crystallographic relation to mullite with oxygen partial pressure. Figure 12 shows a typical TEM image of ϵ - Fe_2O_3 particles in N9802. Dendritic fin-like ϵ - Fe_2O_3 crystals grow epitaxially to ca. $0.3 \times 0.1 \times 0.8 \mu\text{m}^3$. The ED pattern shows that the $[3\bar{1}0]$ zone axis (or $[\bar{1}30]$ zone axis) for mullite and the $[001]$ zone axis for ϵ - Fe_2O_3 correspond to each other, indicating that $c_m \perp (110)_\epsilon$ and $(130)_m$ (or $(310)_m // (\bar{1}\bar{3}0)_\epsilon$, which is con-

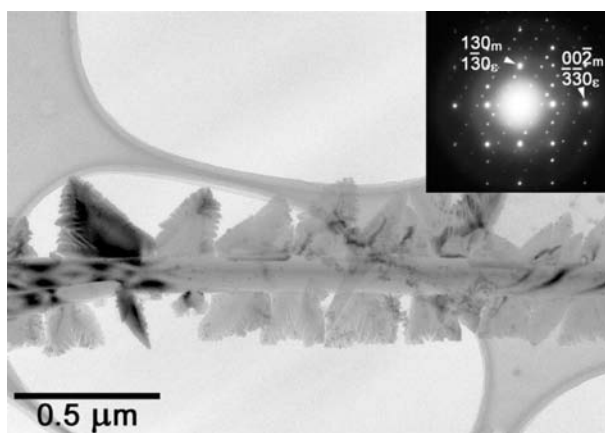


FIGURE 12. Typical TEM image of ε - Fe_2O_3 particles in N98O2. Dendritic fin-like ε - Fe_2O_3 crystals grow epitaxially on a mullite crystal.

sistent with the numerical relations of $3c_m \approx 2d_{(110)_e}$ and $d_{(130)_m}$ (or $d_{(310)_m} \approx d_{(130)_e}$). Note that it was not possible to discriminate between a_m and b_m within the experimental error.

The ε - Fe_2O_3 particles received little attention compared with α - and γ - Fe_2O_3 until they were identified as a potentially useful magnetic material.^{26–31} We hope that continued study of the *hidasuki* color formation may reveal sophisticated processes to achieve fine morphological control of ε - Fe_2O_3 particles.

Applications

One of the aims of this study was to provide potters with new inspirations, by providing information that would enable them to control the formation of the *hidasuki* color and thus produce new and exciting works. As a first step toward achieving this goal, an attempt was made to artificially create a carefully controlled *hidasuki* pattern without the use of rice straw. The results are shown in Figure 13, where the left and right pellets show the Chinese characters for *wabi* (richness and beauty in simplicity and poverty) and *sabi* (aesthetic sense of loneliness), respectively. To produce them, the characters on the surface of the Bizen clay pellets were handwritten using a brush soaked in ethyl alcohol containing a homogeneous dispersion of potassium chloride. The pellets were then heated to 1250 °C at a rate of 1 °C/min and cooled to 800 °C at a rate of 1 °C/min in air.

We also attempted to create a new type of pigment that would also result in properties similar to *hidasuki*. Soda-lime glass containing 1.1 wt % iron(II) was synthesized, and the glass was then mixed with 50 wt % corundum. The mixture was heated at 1250 °C for 2 h and then cooled to 800 °C at a rate of 5 °C/min in air, resulting in the yellowish red solid shown in Figure 14a. As expected, hematite crystals were

(a) Before heating



Wabi

Sabi

(b) After heating



FIGURE 13. Artificial *hidasuki* pattern drawn in the form of handwritten Chinese characters: left, *wabi*; right, *sabi*.



FIGURE 14. Yellowish red powder synthesized from iron containing glass and corundum: (a) as prepared; (b) heated at 1100 °C for 2 h in air.

grown epitaxially on the corundum crystals in the powder particles. This new pigment is also free from hazardous materials such as Cr and Pb, and the color does not change after 2 h heat treatment at 1100 °C in air, as shown in Figure 14b. As a result, we believe that this may offer a useful alternative to some commonly used pigments that contain hazardous materials or are less stable at high temperatures.

Summary and Outlook

The principles of solid state chemistry were applied to investigate the coloring mechanism of Bizen stoneware, which is one of the most popular ceramic art forms in Japan. Control of the reddish *hidasuki* coloring of this stoneware has traditionally been the secret of the master potter; a secret only revealed to apprentices through years of study and devotion to the art. Using modern techniques, we have been able to provide artists with a deeper understanding of the color for-

mation process, enabling them to produce even greater and more beautiful works.

Investigation of the color formation process in Bizen stoneware has also revealed some interesting and potentially useful crystal structures that may be useful in fields far removed from that of pottery. Furthermore, we believe that there are many new and interesting structures and phenomena waiting to be discovered through the investigation of traditional techniques and practices.

This study was supported by Grants-in-Aid for Scientific Research (KAKENHI) Nos. 19550199, 17105002, and 21550194.

BIOGRAPHICAL INFORMATION

Yoshihiro Kusano received his Ph.D. degree from Okayama University in 1995. He started his academic career at Kurashiki University of Science and the Arts in 1995. He is a specialist in microscopy. His research interests include science in ceramic arts and also the study of oxide superconductors.

Minoru Fukuhara received his Ph.D. degree from Tokyo Institute of Technology in 1980. He worked as a research associate at Material Research Laboratory, the Pennsylvania State University, until 1981. Since 1981, he has been working at Okayama University of Science. He is currently a professor. His research interests involve slag carbonation.

Jun Takada received his Ph.D. degree from Kyoto University in 1981. After working at Kyoto University as an associate assistant, he has been a professor of Okayama University since 1986. He was the dean of Graduate School of Natural Science and Technology, Okayama University during 2005–2008. His research interests involve iron oxides, biomineralization and science in ceramic arts.

Akira Doi received his Ph.D. degree from Waseda University in 1971. He started his academic career at Okayama University of Science in 1969. He was the president of Kurashiki University of Science and the Arts until 2005. He is currently a professor and a president advisor at Kurashiki University of Science and the Arts. His research interests involve clay science.

Yasunori Ikeda received his Ph. D. degree from Kyoto University in 2007. He was a researcher at the Institute for Chemical Research, Kyoto University, for 45 years until 2008. His research interests include iron oxides, ferrites, and oxide superconductors.

Mikio Takano received his Ph.D. degree in 1973 from Kyoto University. He started his academic career in Konan University but moved to the Institute for Chemical research, Kyoto University, and served as the director of this institute during 2002–2005. He is presently at the Institute for Integrated Cell-Material Sciences, Kyoto University, as a program-specific professor. This institute is one of the five highly prestigious “World Premier International Research Centers” established in October 2007. At the same time, he is the president of the Japan Society of Powder and Powder

Metallurgy. Throughout his academic career he has done solid state chemistry on 3d transition metal oxides.

FOOTNOTES

*To whom correspondence should be addressed. Tel and Fax: +81 86 440 1051. E-mail: yoshi-k@arts.kusa.ac.jp.

REFERENCES

- Nakamura, T.; Taniguchi, Y.; Tsuji, S.; Oda, H. Radiocarbon Dating of Charred Residues on Earliest Pottery in Japan. *Radiocarbon* **2001**, *43*, 1129–1138.
- Leisure and Recreational Activities in Japan*; Japan Productivity Center: Tokyo, 2005, pp 18 (in Japanese).
- Doi, A.; Sakamoto, N.; Tsutsumi, S.; Ohtsuka, R.; Kato, C. Thermal Property of Bizen-yaki Clay. *J. Chem. Soc. Jpn.* **1979**, 71–75 (in Japanese).
- Doi, A.; Fujiwara, M.; Fukuhara, M. The Formation of Corundum on Hidasuki of Bizen-yaki. *J. Chem. Soc. Jpn.* **1988**, 906–910 (in Japanese).
- Fujiwara, M.; Yamaguchi, K.; Fukuhara, M.; Doi, A. Behavior of Iron Oxide in the Heating Process of Bizen-clay and Potassium Chloride Mixture. *J. Chem. Soc. Jpn.* **1989**, 882–883 (in Japanese).
- Fukuhara, M.; Fujiwara, M.; Yamaguchi, K.; Doi, A. Formation of Hematite and Its Effect on the Coloration of Hidasuki on Bizen-yaki. *J. Ceram. Soc. Jpn. Int. Ed.* **1989**, *97*, 1426–1428.
- Yamaguchi, K.; Kusano, Y.; Fukuhara, M.; Doi, A. Behavior of Ion Components in the Heating Process of Potassium Chloride, Iron Oxide (III) and Mullite. *J. Chem. Soc. Jpn.* **1991**, 1073–1077 (in Japanese).
- Yamaguchi, K.; Kusano, Y.; Fukuhara, M.; Doi, A.; Takada, T. Coloration Mechanism of Hidasuki on Bizen-yaki (I). *J. Jpn. Soc. Powder Powder Metall.* **1992**, *39*, 79–85 (in Japanese).
- Yamaguchi, K.; Kusano, Y.; Fukuhara, M.; Doi, A.; Takada, T. Coloration Mechanism of Hidasuki on Bizen-yaki (II). *J. Jpn. Soc. Powder Powder Metall.* **1992**, *39*, 179–183 (in Japanese).
- Takada, T. On the Effects of Particle Size and Shape on the Color of Ferric Oxide Powders. *J. Jpn. Soc. Powder Powder Metall.* **1958**, *4*, 160–168 (in Japanese).
- Takada, T. Studies on Iron Red Glaze. *J. Jpn. Soc. Powder Powder Metall.* **1958**, *4*, 169–186 (in Japanese).
- Brownell, W. E. Subsolidus Relations between Mullite and Iron Oxide. *J. Am. Ceram. Soc.* **1958**, *41*, 226–230.
- Schneider, H.; Rager, H. Iron Incorporation in Mullite. *Ceram. Int.* **1986**, *12*, 117–125.
- Schneider, H. Temperature-Dependent iron Solubility in Mullite. *J. Am. Ceram. Soc.* **1987**, *70*, C-43–45.
- Cardile, C. M.; Brown, I. W. M.; Mackenzie, K. J. D. Mössbauer Spectra and Lattice Parameters of Iron-Substituted Mullites. *J. Mater. Sci. Lett.* **1987**, *6*, 357–362.
- Kusano, Y.; Fukuhara, M.; Fujii, T.; Takada, J.; Murakami, R.; Doi, A.; Anthony, L.; Ikeda, Y.; Takano, M. Microstructure and Formation Process of the Characteristic Reddish Color pattern Hidasuki on Bizen Stoneware: Reactions Involving Rice Straw. *Chem. Mater.* **2004**, *16*, 3641–3646.
- Kusano, Y.; Fukuhara, M.; Doi, A. Reddish Color Pattern Called Hidasuki on Bizen Stoneware. *Ceram. Jpn.* **2006**, *41*, 377–380 (in Japanese).
- Kusano, Y.; Yamaguchi, K.; Fukuhara, M.; Doi, A. Scientific Study of “Hidasuki” Pattern on Bizen Stoneware. *J. Jpn. Soc. Powder Powder Metall.* **2007**, *54*, 75–80 (in Japanese).
- Song, H.; Coble, R. L. Origin and Growth Kinetics of Platelike Abnormal Grains in Liquid-Phase-Sintered Alumina. *J. Am. Ceram. Soc.* **1990**, *73*, 2077–2085.
- Song, H.; Coble, R. L. Morphology of Platelike Abnormal Grains in Liquid-Phase-Sintered Alumina. *J. Am. Ceram. Soc.* **1990**, *73*, 2086–2090.
- Goswami, A. P.; Roy, S.; Mitra, M. K.; Das, G. C. Impurity-Dependent Morphology and Grain in Liquid-Phase-Sintered Alumina. *J. Am. Ceram. Soc.* **2001**, *84*, 1620–1626.
- Sciau, P.; Relaix, S.; Roucau, C.; Kihn, Y.; Chabanne, D. Microstructural and Microchemical Characterization of Roman Period Terra Sigillata Slips from Archaeological Sites in Southern France. *J. Am. Ceram. Soc.* **2006**, *89*, 1053–1058.
- Sciau, P.; Relaix, S.; Mirguet, C.; Goudeau, P.; Bell, A. M. T.; Jones, R. L.; Pantos, E. Synchrotron X-Ray Diffraction Study of Phase Transformations in Illitic Clays to Extract Information on Sigillata Manufacturing Process. *Appl. Phys. A: Mater. Sci. Process.* **2008**, *90*, 61–66.
- Kusano, Y.; Doi, A.; Fukuhara, M.; Nakanishi, M.; Fujii, T.; Takada, J.; Ikeda, Y.; Takano, M. Effects of Rice Straw on the Color and Microstructure of Bizen, a Traditional Japanese Stoneware, as a Function of Oxygen Partial Pressure. *J. Am. Ceram. Soc.* **2009**, *92*, 1840–1844.

- 25 Kusano, Y.; Fujii, T.; Takada, J.; Fukuhara, M.; Doi, A.; Ikeda, Y.; Takano, M. Epitaxial Growth of ϵ -Fe₂O₃ on Mullite Found through Studies on a Traditional Japanese Stoneware. *Chem. Mater.* **2008**, *20*, 151–156.
- 26 Dézsi, I.; Coey, J. M. D. Magnetic and Thermal Properties of ϵ -Fe₂O₃. *Phys. Status Solidi* **1973**, *15*, 681–685.
- 27 Tronc, T.; Chanéac, C.; Jolivet, J. P. Structural and Magnetic Characterization of ϵ -Fe₂O₃. *J. Solid State Chem.* **1998**, *139*, 93–104.
- 28 Dormann, J. L.; Viart, N.; Rehspringer, J. L.; Ezzir, A.; Niznansky, D. Magnetic Properties of Fe₂O₃ Particles Prepared by Sol-Gel Method. *Hyperfine Interact.* **1998**, *112*, 89–92.
- 29 Jin, J.; Ohkoshi, S.; Hashimoto, K. Giant Coercive Field of Nanometer-Sized Iron Oxide. *Adv. Mater.* **2004**, *16*, 48–51.
- 30 Gich, M.; Roig, A.; Frontera, C.; Moling, E.; Sort, J.; Popovici, M.; Chouteau, G.; Martín y Marero, D.; Nogués, J. Large Coercivity and Low-Temperature Magnetic Reorientation in ϵ -Fe₂O₃ Nanoparticles. *J. Appl. Phys.* **2005**, *98*, 044307.
- 31 Kurmoo, M.; Rehspringer, J. L.; Hutlova, A.; D'Orléans, C.; Vilminot, S.; Estournès, C.; Niznansky, D. Formation of Nanoparticles of ϵ -Fe₂O₃ from Yttrium Iron Garnet in a Silica Matrix: An Unusually Hard Magnet with a Morin-Like Transition below 150 K. *Chem. Mater.* **2005**, *17*, 1106–1114.